

Preparation of SnO₂/Carbon Composite Hollow Spheres and Their Lithium Storage Properties

Xiong Wen Lou,^{*,†,‡} Da Deng,[§] Jim Yang Lee,[§] and Lynden A. Archer^{*,†}

School of Chemical and Biomolecular Engineering, Cornell University, Ithaca, New York 14853-5201, School of Chemical and Biomedical Engineering, Nanyang Technological University, 70 Nanyang Avenue, Singapore 637457, Singapore, and Department of Chemical and Biomolecular Engineering, National University of Singapore, 10 Kent Ridge Crescent, Singapore 119260, Singapore

Received June 13, 2008. Revised Manuscript Received July 31, 2008

In this work, we present a novel concept of structural design for preparing functional composite hollow spheres and derived double-shelled hollow spheres. The approach involves two main steps: preparation of porous hollow spheres of one component and deposition of the other component onto both the interior and exterior surfaces of the shell as well as in the pores. We demonstrate the concept by preparing SnO₂/carbon composite hollow spheres and evaluate them as potential anode materials for lithium-ion batteries. These SnO₂/carbon hollow spheres are able to deliver a reversible Li storage capacity of 473 mA h g⁻¹ after 50 cycles. Unusual double-shelled carbon hollow spheres are obtained by selective removal of the sandwiched porous SnO₂ shells.

Introduction

As energy storage devices, lithium ion batteries (LIBs) are the dominant power source for portable consumer electronics, and their performance is approaching the limit achievable with current electrode materials.^{1,2} The ever-growing need for high capacity and/or high power, especially for emerging large-scale applications (e.g., electric cars and power backup), has prompted numerous research efforts aimed at developing new high-performance electrode materials for next-generation LIBs.^{3–6} Tin-based materials have attracted particular interest as negative electrodes because they can in principle deliver much higher specific lithium storage capacities (790 mA h g⁻¹ for SnO₂; 990 mA h g⁻¹ for Sn) than the currently used graphite materials (372 mA h g⁻¹).^{2,3,7–9} However, the practical use of tin-based anodes is significantly hampered by the poor capacity retention over long-term charge–discharge cycling.¹ This problem is common to anode materials based on the Li-metal alloying/

dealloying mechanism and has been known to arise mainly from the large volume change of electrode materials accompanying Li insertion and extraction (e.g., the volume change is more than 200% when Sn alloys with Li to form Li_{4.4}Sn),¹⁰ which causes disintegration and hence degeneration of conduction pathways between adjacent particles.¹ To alleviate this pulverization so-called problem and further enhance the structural stability, one effective strategy is to design the nanostructure of electrode materials.^{3,5,11} For example, hollow and/or porous nanostructures are shown to be advantageous, where the idea is to use the local empty space to partially accommodate the large volume change.^{12–20} Another commonly used approach is to make nanocomposite materials (e.g., the inactive/active concept),¹ particularly with carbon, where the function of carbon is twofold: providing a physical buffering layer for the large volume change (cushion effect) and increasing the electrical conductivity.^{7,9,14,21–23}

* Corresponding authors. E-mail: laa25@cornell.edu (L.A.A.); xwlou@ntu.edu.sg (X.W.L.).

[†] Cornell University.

[‡] Nanyang Technological University.

[§] National University of Singapore.

- (1) Tarascon, J. M.; Armand, M. *Nature* **2001**, *414*, 359.
- (2) Idota, Y.; Kubota, T.; Matsufuji, A.; Maekawa, Y.; Miyasaka, T. *Science* **1997**, *276*, 1395.
- (3) Hassoun, J.; Panero, S.; Simon, P.; Taberna, P. L.; Scrosati, B. *Adv. Mater.* **2007**, *19*, 1632.
- (4) Nam, K. T.; Kim, D. W.; Yoo, P. J.; Chiang, C. Y.; Meethong, N.; Hammond, P. T.; Chiang, Y. M.; Belcher, A. M. *Science* **2006**, *312*, 885.
- (5) Taberna, L.; Mitra, S.; Poizot, P.; Simon, P.; Tarascon, J. M. *Nat. Mater.* **2006**, *5*, 567.
- (6) Kang, K.; Meng, Y. S.; Breger, J.; Grey, C. P.; Ceder, G. *Science* **2006**, *311*, 977.
- (7) Derrien, G.; Hassoun, J.; Panero, S.; Scrosati, B. *Adv. Mater.* **2007**, *19*, 2336.
- (8) Park, M. S.; Wang, G. X.; Kang, Y. M.; Wexler, D.; Dou, S. X.; Liu, H. K. *Angew. Chem., Int. Ed.* **2007**, *46*, 750.
- (9) Noh, M.; Kwon, Y.; Lee, H.; Cho, J.; Kim, Y.; Kim, M. G. *Chem. Mater.* **2005**, *17*, 1926.

- (10) Larcher, D.; Beattie, S.; Morcrette, M.; Edstroem, K.; Jumas, J. C.; Tarascon, J. M. *J. Mater. Chem.* **2007**, *17*, 3759.
- (11) Guo, Y. G.; Hu, Y. S.; Sigle, W.; Maier, J. *Adv. Mater.* **2007**, *19*, 2087.
- (12) Lou, X. W.; Archer, L. A.; Yang, Z. C. *Adv. Mater.* **2008**, in press (an invited review article).
- (13) Lou, X. W.; Wang, Y.; Yuan, C.; Lee, J. Y.; Archer, L. A. *Adv. Mater.* **2006**, *18*, 2325.
- (14) Wang, Y.; Zeng, H. C.; Lee, J. Y. *Adv. Mater.* **2006**, *18*, 645.
- (15) Lou, X. W.; Deng, D.; Lee, J. Y.; Feng, J.; Archer, L. A. *Adv. Mater.* **2008**, *20*, 258.
- (16) Ma, H.; Cheng, F. Y.; Chen, J.; Zhao, J. Z.; Li, C. S.; Tao, Z. L.; Liang, J. *Adv. Mater.* **2007**, *19*, 4067.
- (17) Han, S. J.; Jang, B. C.; Kim, T.; Oh, S. M.; Hyeon, T. *Adv. Funct. Mater.* **2005**, *15*, 1845.
- (18) Lou, X. W.; Archer, L. A. *Adv. Mater.* **2008**, *20*, 1853.
- (19) Lee, K. T.; Jung, Y. S.; Oh, S. M. *J. Am. Chem. Soc.* **2003**, *125*, 5652.
- (20) Demir-Cakan, R.; Hu, Y. S.; Antonietti, M.; Maier, J.; Titirici, M. M. *Chem. Mater.* **2008**, *20*, 1227.
- (21) Wen, Z. H.; Wang, Q.; Zhang, Q.; Li, J. H. *Adv. Funct. Mater.* **2007**, *17*, 2772.
- (22) Ng, S. H.; Wang, J. Z.; Wexler, D.; Konstantinov, K.; Guo, Z. P.; Liu, H. K. *Angew. Chem., Int. Ed.* **2006**, *45*, 6896.

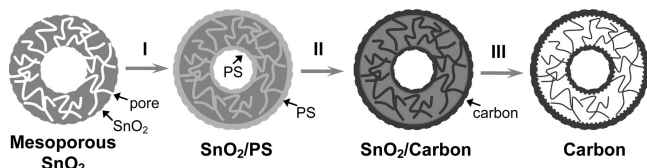


Figure 1. Schematic illustration of the synthetic procedure for SnO₂/carbon composite hollow spheres and derived carbon double-shelled hollow spheres.

As an example, Scrosati and co-workers have recently reported a superior nanostructured Sn–C composite anode material with Sn nanoparticles finely dispersed in a supporting carbon matrix. The synthesis involves the infiltration of an organometallic tin precursor into an organic Resorcinol–Formaldehyde gel followed by calcinations under argon.⁷

Combining the nanostructure design of electrode materials and the nanocomposite concept, we herein report a new hierarchical anode nanostructure: SnO₂/carbon composite hollow spheres. In these structures, the mesoporous SnO₂ hollow spheres are embedded in 3D carbon networks.¹¹ The synthetic procedure of SnO₂/carbon composite hollow spheres is schematically illustrated in Figure 1. In step I, a glucose-derived polysaccharide (PS) carbon precursor is efficiently infiltrated into the mesoporous SnO₂ shells through 3D interconnected “nano-channels” (i.e., pores) and deposited onto both its interior and exterior surfaces. In step II, the PS is carbonized under inert atmosphere to produce a 3D carbon network in the SnO₂ shell sandwiched by two carbon shells.

Experimental Section

Materials Synthesis. In a typical synthesis of mesoporous SnO₂ hollow nanospheres, certain amounts of urea and potassium stannate trihydrate (K₂SnO₃·3H₂O, Aldrich, 99.9%) were dissolved in a mixed solvent of ethanol/water (37.5% ethanol by volume) to achieve concentrations of 0.1 M and 16 mM, respectively. Afterward, the solution was transferred to Teflon lined stainless steel autoclaves and hydrothermally treated in an air-flow electric oven at 150 °C for 24 h to produce a white precipitate, which was then harvested by centrifugation and washed with ethanol and deionized water followed by vacuum drying at room temperature. To prepare SnO₂/polysaccharide composite hollow spheres, 0.2 g of as-synthesized mesoporous SnO₂ hollow nanospheres was easily dispersed by ultrasonication in 20 mL of 1.0 M aqueous glucose solution. The suspension was transferred to a 40 mL Teflon lined autoclave, which was then heated in an air-flow electric oven at 180 °C for 3 h. The product was again harvested by centrifugation and washed with deionized water and ethanol at least five times. After drying at 50 °C, the resulting brown powder was carbonized at 550 °C for 3 h under inert atmosphere to obtain SnO₂/carbon composite hollow spheres.

Materials Characterization. Products were thoroughly characterized with X-ray powder diffraction (XRD; Scintag PAD X, Cu Kα, λ = 1.5406 Å), field emission scanning electron microscopy (FESEM; Hitachi S4500), and transmission electron microscopy (TEM; JEOL-1200EX, 120 kV, and FEI Tecnai T12, 120 kV). The nitrogen adsorption and desorption isotherm was measured using Micromeritics ASAP 2020 sorptometer.

Electrochemical Measurement. The electrochemical measurements were carried out using homemade two-electrode cells with

lithium metal as the counter and reference electrodes at room temperature. The working electrode consisted of active material (e.g., SnO₂/carbon composite hollow spheres), conductivity agent (carbon black, Super-P), and polymer binder (polyvinylidene difluoride, PVDF, Aldrich) in a weight ratio of around 80:10:10. The electrolyte was 1 M LiPF₆ in a 50:50 (w/w) mixture of ethylene carbonate and diethyl carbonate. Cell assembly was carried out in an Ar-filled glovebox with the concentrations of moisture and oxygen below 1 ppm. Charge–discharge cycles of the cells were measured between 2.0 and 0.005 V at a constant current density of 100 mA/g based on the active material with a Maccor-Series-2000 battery tester. Similar measurement was also carried out for pure SnO₂ hollow nanospheres at a current rate of 160 mA/g.

Results and Discussion

As shown in Figure 2a–d the mesoporous SnO₂ hollow spheres with size in the range of 150–400 nm are prepared by a template-free route based on an inside-out Ostwald ripening mechanism.^{12,13} Since the hollow interior space is created by spontaneous evacuation of the interior materials through the shell, it follows that the as-formed SnO₂ shell must be highly porous. Here we confirm this structural feature by N₂ sorption measurements. As shown in Figure 2e, the N₂ adsorption–desorption isotherm is characteristic of type IV with a relatively unusual type H4 hysteresis loop, which might appear to be a unique characteristic of large pores (the hollow interior) embedded in a matrix with pores of much smaller sizes (the mesoporous shell).²⁴ Figure 2f shows the corresponding pore size distributions calculated by the Barrett–Joyner–Halenda (BJH) method from both adsorption and desorption branches. Most notably, there is a sharp peak around 4 nm in the pore size distribution from the desorption branch. In general, pore size distribution from the desorption branch is less reliable,²⁴ and such a sharp peak should be treated with caution: it may be an artifact corresponding to capillary evaporation at the lower end of the hysteresis loop with a relative pressure of about 0.4–0.5. Nonetheless, from the pore size distributions, it can be concluded that the pores are generally smaller than 5 nm. As expected, such a mesoporous structure gives rise to a relatively high Brunauer–Emmett–Teller (BET) specific surface area of about 110 m²/g.

The pores of the SnO₂ shells are large enough to be directly infiltrated with carbon precursor (PS) derived from glucose under hydrothermal conditions.²⁵ Previously this simple method has been employed to coat carbon material on a variety of nanoparticles and to deposit carbon in amino-functionalized silica pores of a few nanometers.^{9,25–27} Unlike other commonly used polymer carbon precursors (e.g., polyacrylonitrile, PAN),^{7,28} glucose-derived PS enables facile integration of carbon to nanostructure synthesis in solution,²⁷ and most importantly it can be carbonized at a temperature as low as 400 °C.²⁶ It is reported that tin oxide could be carbothermally reduced to metallic tin when the carbonization

(24) Kruk, M.; Jaroniec, M. *Chem. Mater.* **2001**, *13*, 3169.

(25) Ikeda, S.; Tachi, K.; Ng, Y. H.; Ikoma, Y.; Sakata, T.; Mori, H.; Harada, T.; Matsumura, M. *Chem. Mater.* **2007**, *19*, 4335.

(26) Sun, X. M.; Liu, J. F.; Li, Y. D. *Chem. Mater.* **2006**, *18*, 3486.

(27) Sun, X. M.; Li, Y. D. *Angew. Chem., Int. Ed.* **2004**, *43*, 597.

(28) Lee, J.; Kim, J.; Hyeon, T. *Adv. Mater.* **2006**, *18*, 2073.

(23) Park, M. S.; Needham, S. A.; Wang, G. X.; Kang, Y. M.; Park, J. S.; Dou, S. X.; Liu, H. K. *Chem. Mater.* **2007**, *19*, 2406.

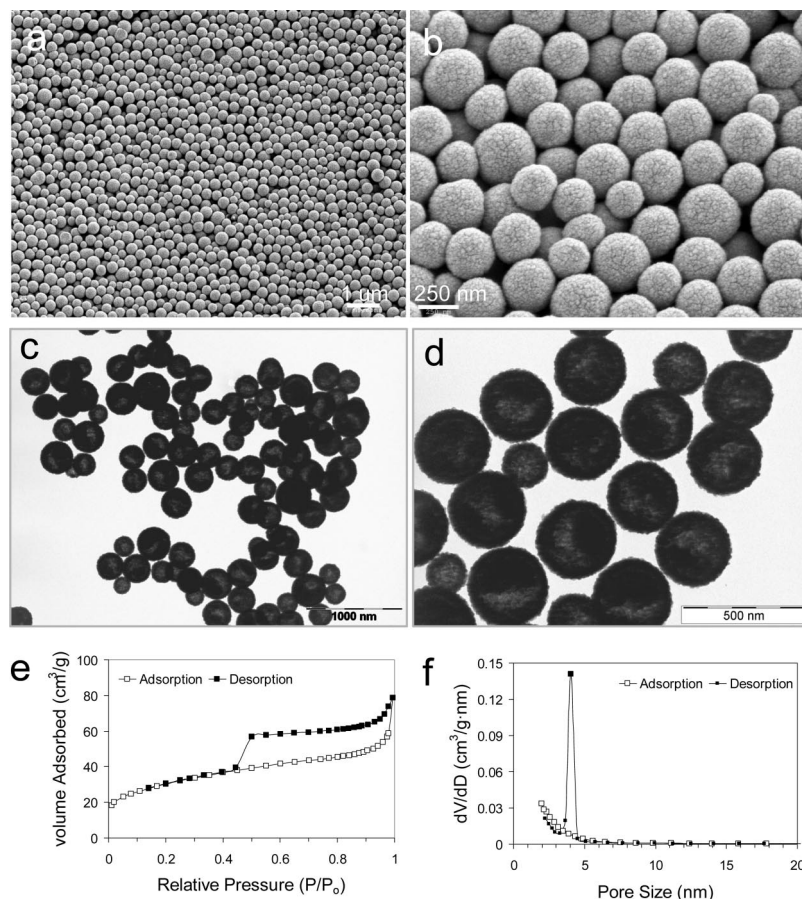


Figure 2. Characterization of SnO_2 hollow nanospheres: SEM (a, b) and TEM (c, d) images; (e) N_2 adsorption–desorption isotherm at 77 K; (f) corresponding pore size distributions calculated by BJH method from both branches.

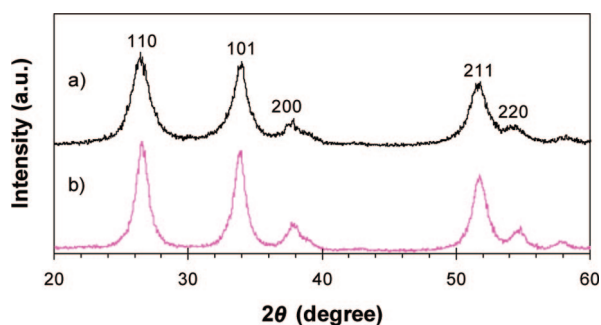


Figure 3. XRD patterns of SnO_2 hollow nanospheres (a) and SnO_2 /carbon composite hollow spheres (b).

temperature reaches 600 °C.²⁶ Because of the very low melting temperature of tin (322 °C), it will evaporate once formed at a much higher temperature, which is verified in experiments carried out at temperatures above 600 °C. Indeed, our initial attempt to incorporate carbon networks from a polymer precursor (e.g., PAN) by vapor deposition polymerization^{29,30} has proven to be unfruitful. Therefore, in this work carbonization is carried out at 550 °C to avoid destruction of the nanostructure. As confirmed by X-ray diffraction (XRD) analysis (Figure 3b) no elemental Sn is formed after carbonization at 550 °C while the SnO_2 peaks are slightly sharpened as compared to the XRD pattern of the pristine SnO_2 hollow spheres (Figure 3a).

The morphology and microstructure of the as-synthesized SnO_2 /carbon nanocomposite are examined with scanning electron microscopy (SEM) and transmission electron microscopy (TEM). From the SEM image shown in Figure 4a the overall morphology of SnO_2 /carbon composite is very similar to that of SnO_2 hollow spheres. To determine the carbon content in the SnO_2 /carbon composite, thermogravimetric analysis (TGA) is carried out. Figure 4b shows the TGA curve under air with a temperature ramp of 10 °C/min. From the observation that the TGA curve is monotonic and the weight loss mainly takes place below 600 °C, one can rule out the possible carbothermal reduction of SnO_2 and reoxidation of Sn by oxygen (recall the above XRD analysis and discussion about carbothermal reduction). Therefore, the carbon content in the SnO_2 /carbon nanocomposite is simply determined to be about 33.5% by weight. The hollow spherical nature of these SnO_2 /carbon composite particles is clearly revealed by the low-magnification TEM image (Figure 4c), although it is difficult to observe a layer of carbon coating due to the high contrast of the image. Figure 4d shows a TEM image displaying a representative single hollow sphere. From the relative light contrast, it can be clearly observed that a thin carbon layer is coated uniformly on the outer surface of the SnO_2 sphere. It is further proven that the carbon precursor deposits not only on the outer surface but also penetrates into the mesoporous SnO_2 shell. When the particles are irradiated by focused electron beams during the TEM examination, SnO_2 could

(29) McCann, J. T.; Lim, B. K.; Ostermann, R.; Rycenga, M.; Marquez, M.; Xia, Y. N. *Nano Lett.* **2007**, *7*, 2470.

(30) Johnson, S. A.; Ollivier, P. J.; Mallouk, T. E. *Science* **1999**, *283*, 963.

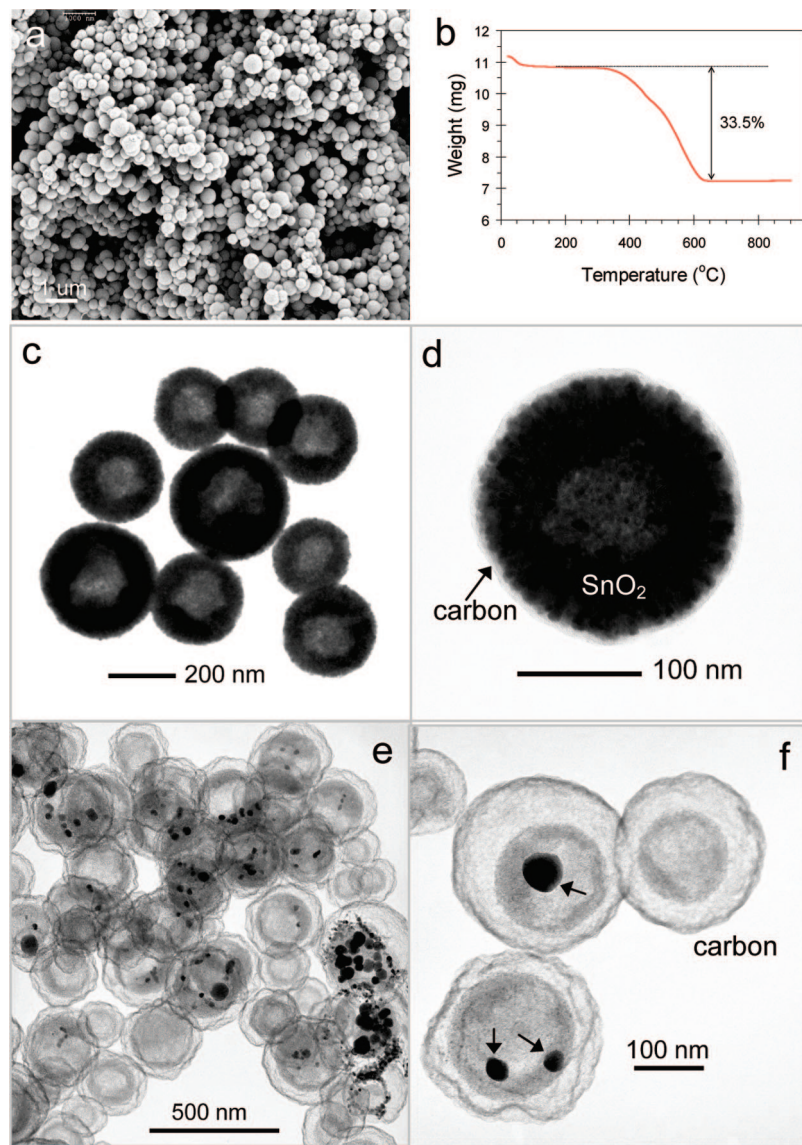


Figure 4. Characterization of SnO₂/carbon composite hollow spheres: (a) SEM image; (b) TGA curve under air with a ramp of 10 °C/min; (c, d) TEM images; (e, f) TEM images showing double-shelled carbon hollow spheres after focused electron beam irradiation. Some remaining Sn nanoparticles are indicated by black arrows in (f).

be reduced to form melted metallic Sn, which could evaporate easily under vacuum.^{26,31} As a result, it is interesting to occasionally observe that double-shelled carbon spheres (Figure 4e,f) are formed in situ upon electron irradiation. Similarly, the mesoporous SnO₂ shells could also be selectively removed by thermal reduction with H₂ and evaporation to prepare the interesting double-shelled carbon hollow spheres as illustrated in Figure 1 (step III).^{32–34} Encapsulated tin nanoparticles can still be observed in some double-shelled hollow spheres (black dots as indicated by black arrows in Figure 4f). Evidently, the observation of the inner carbon shell indicates that the carbon precursor must have infiltrated through the mesoporous SnO₂ shell.

The lithium storage properties of these SnO₂/carbon hollow spheres as a potential anode material for LIBs are evaluated

using a two-electrode cell, where SnO₂/carbon serves as the working electrode and lithium metal serves as the counter and reference electrode.¹³ The reaction mechanism for SnO₂/Li cell can be described as follows: $\text{SnO}_2 + 4\text{Li}^+ + 4\text{e}^- \rightarrow \text{Sn} + 2\text{Li}_2\text{O}$ (1); $\text{Sn} + x\text{Li}^+ + x\text{e}^- \leftrightarrow \text{Li}_x\text{Sn}$ ($0 \leq x \leq 4.4$) (2).^{8,20} Figure 5a,b shows the results in terms of the discharge–charge voltage profiles for the first two cycles and cycling performance (i.e., capacity retention vs cycle number) at a constant current density of 100 mA/g. The voltage profiles are characteristic of SnO₂-based materials.¹³ The initial discharge and charge capacities are 2157 and 983 (mA h)/g, respectively. This large initial irreversible loss (56.3%) is common for SnO₂ materials,^{8,13,20} which is attributed to the irreversible reduction of SnO₂ to Sn as described in eq 1 and other possible irreversible processes, such as decomposition of electrolyte to form a protective film on the electrode surface.^{1,7} From the cycling performance plot (Figure 5b), it is important to note that the capacity tends to level off after 30 cycles and the SnO₂/

(31) Wang, Y.; Lee, J. Y. *J. Nanopart. Res.* **2006**, *8*, 1053.

(32) Lou, X. W.; Yuan, C.; Archer, L. A. *Adv. Mater.* **2007**, *19*, 3328.

(33) Yang, M.; Ma, J.; Zhang, C. L.; Yang, Z. Z.; Lu, Y. F. *Angew. Chem., Int. Ed.* **2005**, *44*, 6727.

(34) Lou, X. W.; Yuan, C.; Archer, L. A. *Small* **2007**, *3*, 261.

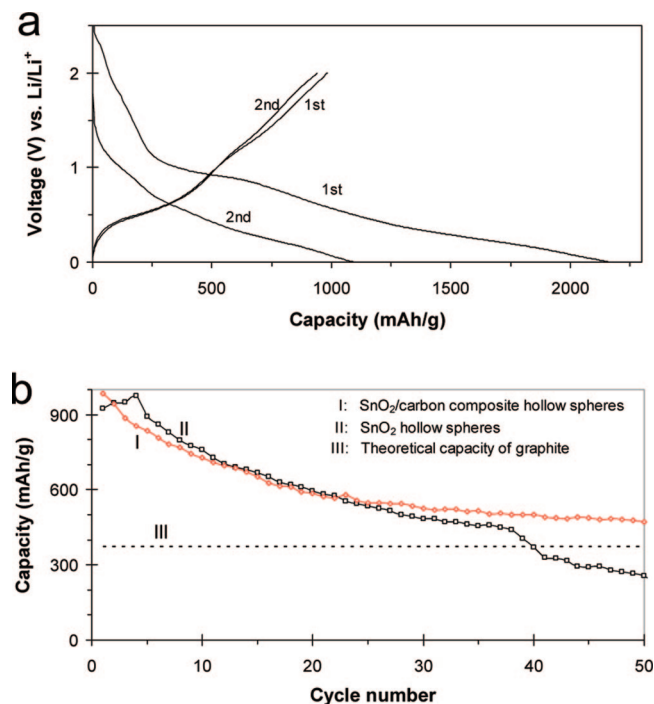


Figure 5. (a) Discharge–charge voltage profiles of $\text{SnO}_2/\text{carbon}$ composite hollow spheres for 1st and 2nd cycles at a current density of 100 mA/g. (b) Cycling performance of $\text{SnO}_2/\text{carbon}$ composite hollow spheres at a current density of 100 mA/g and SnO_2 hollow nanospheres at a current density of 160 mA/g.

carbon hollow spheres are able to deliver a reversible Li storage capacity of 473 (mA h)/g after 50 cycles, which is about 27% higher than the theoretical capacity of graphite (372 (mA h)/g). For comparison, the lithium storage properties of pure SnO_2 hollow spheres are also characterized under similar conditions, and the result is shown in Figure 5b. Note that a current density of 160 mA/g is used for pure SnO_2 hollow spheres to take into account the consideration that $\text{SnO}_2/\text{carbon}$ composite hollow spheres contain about 33.5 wt % of carbon which is barely active for lithium storage,^{7,9,26} although the effect of current rates in such a moderate range on cycling performance is very limited. In agreement with literature works, the capacity of the pure SnO_2 anode tends to fade quickly after 30 cycles to a value below 372 (mA h)/g.^{8,17} It should also be noted that the capacity of the $\text{SnO}_2/\text{carbon}$ composite anode is comparable to that of SnO_2 in

the course of the first 30 cycles, despite the fact that one-third of its mass is composed of low-activity amorphous carbon.^{7,9,26} This observation suggests that the introduction of a carbon matrix to form a truly mixed nanocomposite increases the utilization efficiency of the active component and improves the cycle life of Li-metal alloying electrodes by reducing the pulverization problem.

As a final remark, we point out that the extent of improvement in capacity retention is below our expectation presumably because of two factors: carbon materials completely fill in the pores, and the central cavity is too small (in other words, the shell is too thick). By further tailoring the hollow structures of SnO_2 ,³⁴ a similar concept has nonetheless been successfully applied to prepare composite materials with stable lithium storage capacity retention for hundreds of cycles.³⁵

Conclusions

In summary, we have designed a new nanostructured $\text{SnO}_2/\text{carbon}$ composite anode material with hollow spherical structure. 3D carbon networks in nanoscale can be effectively integrated into mesoporous SnO_2 shells by selective infiltration of carbon precursor in solution followed by carbonization. Interesting double-shelled carbon hollow spheres can be obtained by selective removal of the sandwiched mesoporous SnO_2 shells. The carbon networks act as both physical buffering cushion for the intrinsic large volume change and electrical conducting path. As a result, the capacity retention of the composite electrode is largely improved. The electrode design presented in this work, combining the nanostructure design and composite concept, should be applicable for preparation of other electrode materials.

Acknowledgment. The authors are grateful to the National Science Foundation (Grant No. DMR 0404278) and to the KAUST-CU Center for Energy and Sustainability for supporting this study. Facilities available through the Cornell Center for Materials Research (CCMR) and Cornell Integrated Microscopy Center (CIMC) were used for this study.

CM801607E

(35) Lou, X. W.; Archer, L. A. Unpublished results, 2008.